ACS Partner Journal

ENVIRONMENT & HEALTH

pubs.acs.org/EnvHealth

Article

Benchmark Dose Estimation from Transcriptomics Data for Methylimidazolium Ionic Liquid Hepatotoxicity: Implications for Health Risk Assessment of Green Solvents

Qing Yang,[⊥] Xiaole Zhao,[⊥] Kejia Wu, Qingqing Yu, Qiao Wang, Jingguang Li, Yongning Wu, and Xin Liu*

Cite This: *Environ. Health* 2025, 3, 373−379

Read Online

ACCESS | Metrics & More | Article Recommendations | Supporting Information

ABSTRACT: Ionic liquids (ILs), traditionally considered environmentally benign solvents, have shown potential toxicity to organisms, raising concerns about their safety. Among them, 1-octyl-3-methylimidazolium (M8OI) has been detected at high concentrations in soils and exhibits hepatotoxic properties. To uncover the molecular mechanisms underlying this toxicity, whole-transcriptome sequencing was performed, coupled with benchmark dose (BMD) modeling, to derive transcriptomic points-of-departure (tPOD) through dose−response analysis. The transcriptomic analysis identified 425, 667, and 567 differentially expressed genes (DEGs) following low (10 μmol/L), medium (50 μmol/L), and high (200 μmol/L) doses of M8OI exposure, respectively. Enrichment analysis revealed significant perturbations in pathways related to cytokine−cytokine receptor interaction and IL-17 signaling. BMD modeling yielded tPOD values of 1.51 μmol/L (median of the 20 most sensitive genes, omicBMD$_{20}$), 2.98 μmol/L (tenth percentile of all genes, omicBMD$_{10th}$), 6.83 μmol/L (mode of the first peak of all gene BMDs, omicBMD$_{mode}$), and 5.9 μmol/L for pathway-level analysis. These transcriptomics-derived tPODs were at least 105-fold lower than M8OI's hepatotoxic concentration, as indicated by its EC$_{50}$ of 723.6 μmol/L in HepG2 cells. Functional analysis of the transcriptomic data identified legionellosis, rheumatoid arthritis, and transcriptional misregulation in cancer as the most sensitive pathways affected by M8OI. These findings highlight the molecular mechanisms driving M8OI-induced hepatotoxicity and underscore the utility of transcriptomics in deriving sensitive and quantitative toxicity thresholds. The results provide critical insights for guideline-driven toxicological evaluations and regulatory decision-making, supporting a more comprehensive assessment of IL safety.

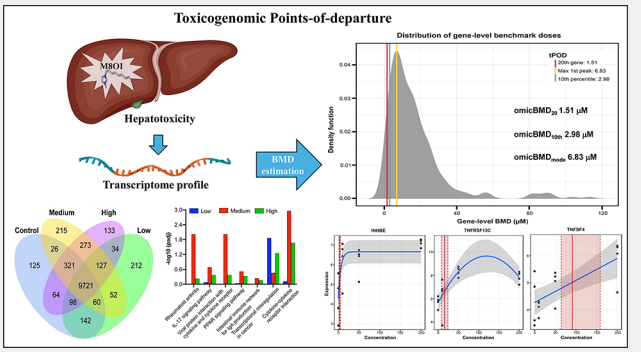

KEYWORDS: *Ionic liquids, 1-Octyl-3-methylimidazolium, Hepatotoxic, Transcriptomics, Benchmark dose*

1. INTRODUCTION

Ionic liquids (ILs) are a unique class of organic salts with distinctive physicochemical properties. They are nonflammable, exhibit negligible vapor pressure, and possess high thermal and chemical stability. Additionally, ILs demonstrate excellent solubility in both aqueous and lipid environments.[1,2] These characteristics make them ideal as environmentally safe "green solvents" for various pharmaceutical, physical, and chemical processes.[3,4] As such, ILs have garnered recognition as a "quiet revolution in materials science" due to their potential to replace volatile organic solvents.[5] It is foreseeable that their utilization, along with consequent release into the environment and subsequent human exposure, will undergo substantial growth in the near future.[6,7]

Research on ILs has intensified, focusing on their environmental behavior and ecological risks.[8] Recent studies have highlighted the toxicity of ILs to organisms, particularly alkylimidazolium ionic liquids such as 1-octyl-3-methylimidazolium (M8OI). High concentrations of M8OI near landfill sites in the North East of England have the potential to induce an autoimmune liver condition known as primary biliary cholangitis (PBC).[9] Moreover, liver toxicity, characterized by oxidative stress, DNA damage, and mitochondria-mediated apoptosis, has been observed in zebrafish,[10] silver carps,[11] and *Paramisgurnus dabryanus*[12] exposed to M8OI. In rodent liver cells, human cholangiocytes, and hepatocarcinoma cells, M8OI has been found to inhibit mitochondrial oxidative phosphor-

Received: June 19, 2024
Revised: November 18, 2024
Accepted: November 19, 2024
Published: December 12, 2024

ylation, ultimately leading to cell apoptosis.[13−15] Mouse models have also demonstrated that M8OI caused hepatocyte vacuolation and mild liver cholangiopathy.[16] Despite the considerable industrial interest in ILs, the current understanding of their environmental and health impacts remains relatively limited for risk regulation.

Omics technologies, particularly whole transcriptomics, enable comprehensive analysis of molecular changes without requiring prior knowledge of toxicity mechanisms.[17] The transcriptomic Point of Departure (tPOD) method capitalizes on the principle that alterations in gene expression are generally preceded by chronic chemical-induced physiological effects in organisms. These changes can be sensitively measured using transcriptomic techniques.[18] This advancement has led to the introduction of transcriptomic benchmark dose (BMD) analysis, which uses transcriptomic data to pinpoint the lowest doses that induce significant biological changes.[19] Consequently, this approach provides a sophisticated means for hazard assessment and risk management.

Using transcriptomic analyses, we aim to unveil the molecular targets and pathways disrupted by M8OI exposure in human liver cells, exploring its hepatotoxic implications. Additionally, applying transcriptomic BMD analysis to determine the tPODs is essential for hazard evaluation. This approach could provide crucial insights for assessing the risk of M8OI as a potential environmental contaminant.

2. MATERIALS AND METHODS

2.1. Chemicals and Reagents

1-octyl-3-methylimidazole chloride salt (M8OI, purity >98.0%) was purchased from Tokyo Chemical Industry Co., Ltd. (Tokyo, Japan). Fetal bovine serum (FBS) was from Gibco by Thermo Fisher Scientific Inc. (Shanghai, China). Penicillin−streptomycin was from Genom (Hangzhou, China). Dulbecco's modified Eagle medium (DMEM) was purchased from Gibco (Thermo Fisher Scientific Inc., Shanghai, China). The human hepatocyte cells (HepG2 cells) were obtained from the Chinese Academy of Sciences (Cell Biology of Shanghai Institute, Shanghai, China).

2.2. Cell Culture and Exposure Assessment

HepG2 cells were cultured in the DMEM medium supplemented with 1% penicillin/streptomycin and 10% FBS. The cells were seeded at a density of 1 × 10∧6 cells/mL and subsequently exposed to a range of M8OI concentrations from 0 μmol/L to 1200 μmol/L. Cultures were maintained at 37 °C in a 5% CO_2 atmosphere. To determine the half-maximal effective concentration (EC_{50}), the MTT assay (3-(4,5-dimethylthiazol-2-yl)-2,5-diphenyltetrazolium bromide) was conducted, with six biological replicates performed.

2.3. Transcriptomic Analysis

HepG2 cells were exposed to 0, 10, 50, and 200 μmol/L of M8OI for 24 h. Total RNA was extracted using the TRIzol method according to the manufacturer's instructions (Invitrogen, Thermo Fisher Scientific, MA, USA). The quality and concentration of the extracted RNA were assessed using the RNA Nano 6000 Assay Kit of the Bioanalyzer 2100 system (Agilent Technologies, CA, USA). Details of the library preparation are provided in the Supporting Information (SI). Sequencing was conducted on an Illumina NovaSeq platform, generating 150 bp paired-end reads. Raw data were filtered for adapter sequences and low-quality reads, then aligned to the reference genome for *Homo sapiens* (UCSC version hg19) using STAR. StringTie was used for reads quantification and normalization to generate the raw gene count matrix and Transcripts Per Kilobase Per Million mapped reads (TPM) values. After filtration with Cutadapt v 2.10, the high-quality clean reads from all samples were merged and assembled by the Trinity package to construct the unigenes for further analysis.

Differentially expressed genes (DEGs) analysis was conducted as described in the SI. This analysis included Gene Ontology (GO) enrichment and Kyoto Encyclopedia of Genes and Genomes (KEGG) pathway analysis, which are also detailed in the SI. Four biological replicates were performed in the transcriptomic analysis.

2.4. Transcriptomic Benchmark Dose Analysis

FastBMD (https://bio.tools/fastbmd)was utilized for benchmark dose−response analysis of the transcriptomics data,[20] resulting in 14,400 matched features following gene ID annotation. Normalized count estimates were filtered to remove 5% and 10% of genes with the lowest variance and abundance, respectively. Subsequently, a log2 transformation was applied to ensure a consistent and appropriate distribution of expression values. Differential expression analysis retained 723 features that met the established thresholds (log2 fold change ≥1.5; False discovery rate ≤0.05) out of 11,158 genes. To determine the gene-level BMD, eight parametric models (Exp2, Exp3, Exp4, Exp5, Linear, Poly2, Hill, and Power) were fitted to the gene expression profiles. A threshold for lack of fit was set at $P > 0.1$, and a benchmark response (BMR) factor of 1.0 was used. The best-fitting model was selected based on the Akaike Information Criterion (AIC), while poorly performing models were filtered out. The tPOD values were computed based on the distribution of gene-level BMDs (geneBMDs) using the following metrics: (1) $tPOD_{20th}$, calculated as the median of the 20 most sensitive geneBMDs ($omicBMD_{20}$); (2) $tPOD_{10th}$, determined as the 10th percentile of all geneBMDs ($omicBMD_{10th}$); (3) $tPOD_{mode}$, defined as the mode of the first peak geneBMDs ($omicBMD_{mode}$). Ultimately, a pathway-level benchmark dose (pathBMD) was determined. This was achieved through the bootstrapped median calculation of gene-based benchmark doses (geneBMDs) within a specified pathway, necessitating a minimum of three geneBMDs.

2.5. Statistical Analysis

All nonomics data were analyzed using GraphPad Prism version 9.2 (GraphPad Software Inc., San Diego, CA, USA). The results are expressed as the mean ± standard deviation. Statistical comparisons among multiple groups were conducted using one-way analysis of variance (ANOVA). A significance level of $P < 0.05$ was considered statistically significant.

3. RESULTS AND DISCUSSION

3.1. Determination of EC_{50} for M8OI-Induced Liver Cytotoxicity

The MTT assay demonstrated a considerable, dose-dependent cytotoxic impact of M8OI on HepG2 cells after 24 h exposure,

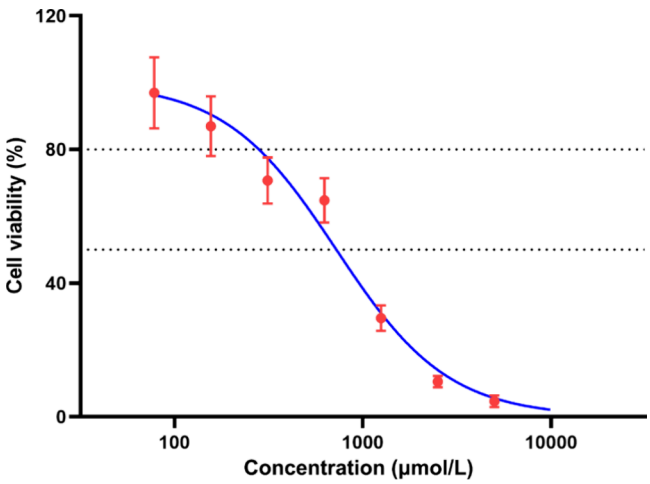

Figure 1. Viabilities of HepG2 cells exposed to various concentrations of M8OI for 24 h.

https://doi.org/10.1021/envhealth.4c00120
Environ. Health 2025, 3, 373−379

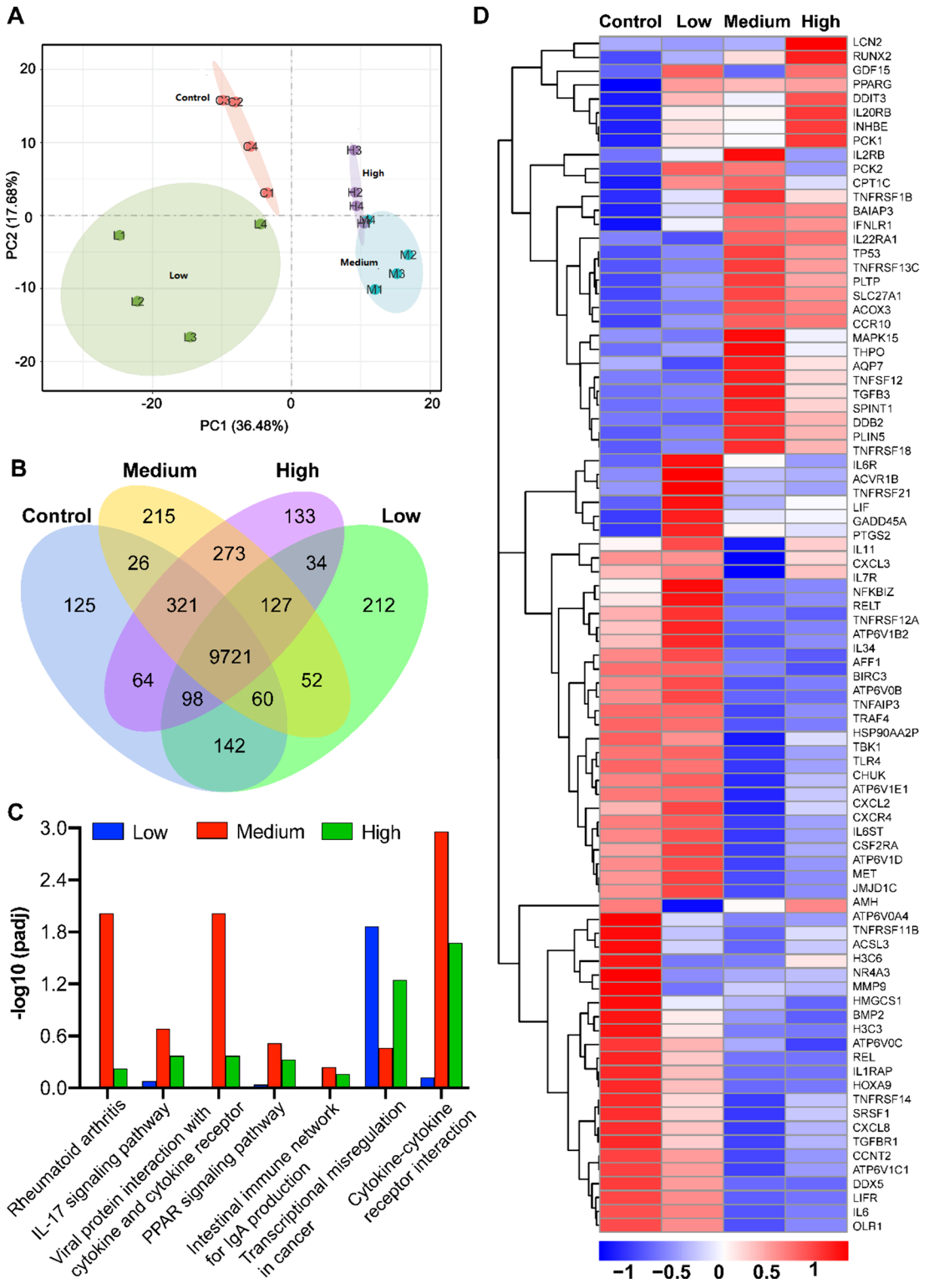

Figure 2. Whole transcript gene alterations in HepG2 cells exposed to M8OI. (A) PCA analysis of each group with four replicates. (B) Venn diagram of differentially expressed transcripts across all concentrations. (C) KEGG pathway enrichment scores of differentially expressed transcripts. (D) Heatmap clustering analysis of the differentially expressed genes.

with an EC_{50} of 723.6 μmol/L (95% confidence interval: 571.4−910.6 μmol/L) (Figure 1). This is distinct from the previously reported EC_{50} of M8OI (as the Br^- salt), which was 439.6 μmol/L in HepG2 cells.[13] This discrepancy is likely due to differences in the anion types of M8OI. Additionally, this observation aligns with the toxicity profiles of M8OI in microorganisms, where [C8mim]Br exhibits greater toxicity than [C8mim]Cl.[21] The primary mechanisms involved in the cellular uptake of ILs include membrane fusion, passive diffusion, and processes mediated by transport proteins.[22,23] The uptake of M8OI into HepG2 cells may occur through several mechanisms, including membrane fusion and transport

https://doi.org/10.1021/envhealth.4c00120
Environ. Health 2025, 3, 373−379

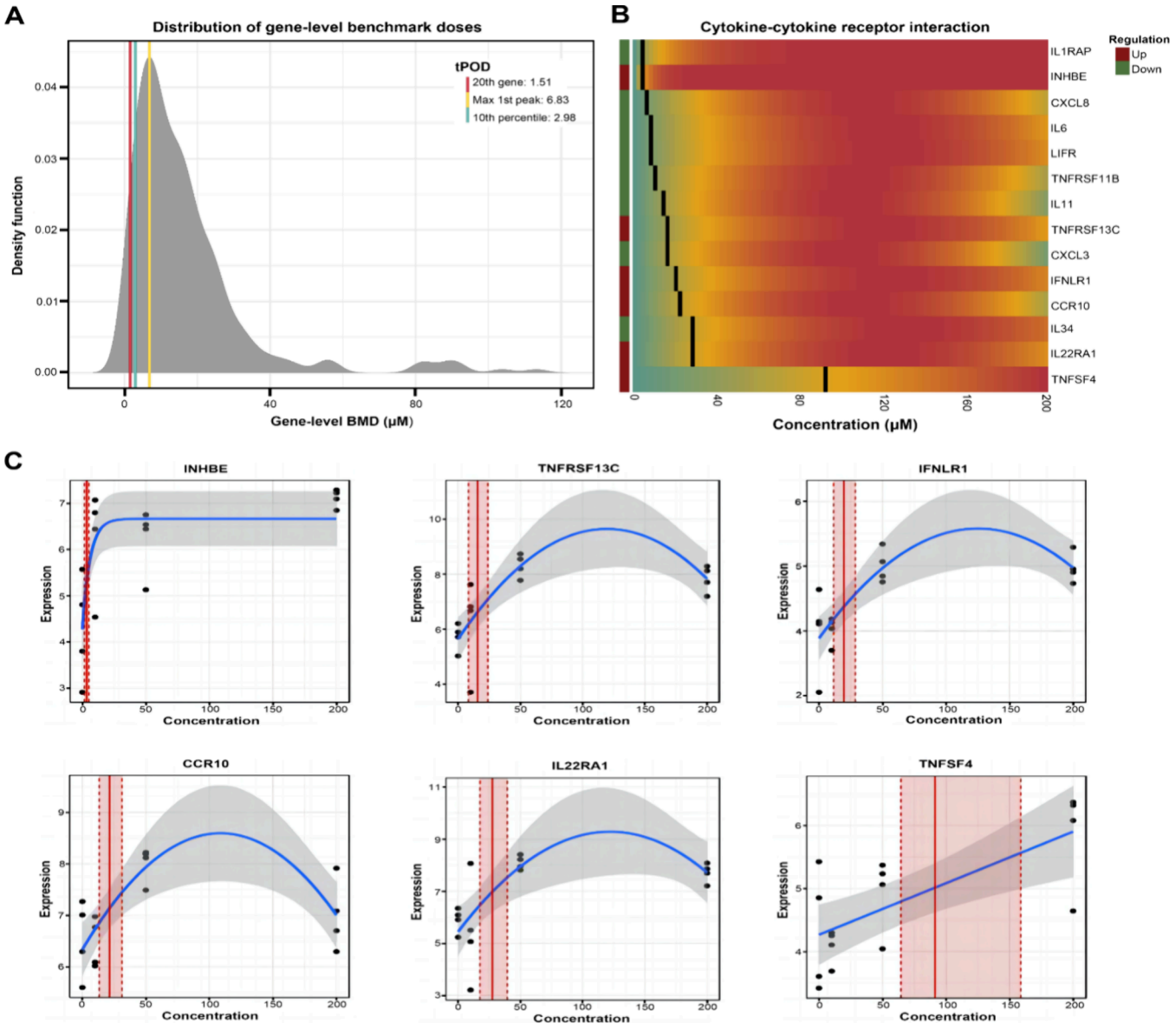

Figure 3. Transcriptome-wide points-of-departure (tPOD) in liver cells exposed to M8OI. (A) Density plot of gene-level BMD; (B) in KEGG pathway enrichment set analysis; (C) Dose−response curve of up-regulated genes in the most sensitive pathway.

protein-mediated processes. Its long alkyl chain (octyl) enhances lipophilicity, thereby facilitating these uptake routes. The dose−response curve was modeled using the equation $[Y = 100/(1 + 10\wedge(\mathrm{LogEC}_{50} - X) * -1.464)]$. Based on this model, the concentration at which cell viability reached 80% was calculated to be 281.0 μmol/L. Consequently, a treatment concentration of 200 μmol/L was selected as the highest dosage for subsequent transcriptomics analysis.

3.2. Transcriptome Profile Alterations in Response to M8OI Exposure

The principal component analysis (PCA) of the full transcriptome data set showed distinct separation based on M8OI exposure dose. Replicates in each group were closely clustered, indicating consistent gene expression responses. Notably, a significant divergence was observed between the control and the M8OI exposure groups (Figure 2A). Exposure to M8OI resulted in the identification of 425, 667, and 567 DEGs in the low, medium, and high dose groups, respectively (Figure 2B). Among these, 127 DEGs were found to overlap across all experimental groups, suggesting a direct association between M8OI exposure and the regulatory mechanisms of these DEGs. The KEGG pathway analysis of the DEGs identified seven key pathways, including the IL-17 signaling pathway, cytokine/cytokine receptor interactions, and the PPAR signaling pathway (Figure 2C). These pathways are known to be involved in the increased reactive oxygen species (ROS) stress response of the liver exposed to hepatotoxins such as PFAS and microplastics.[24−26] These findings indicated that M8OI exposure disrupted the signaling pathways associated with the ROS stress response, thereby inducing hepatotoxic effects. Furthermore, the heatmap profile of differentially expressed transcripts in each group revealed a clear dose-dependent response to M8OI exposure for the majority of DEGs (Figure 2D). These findings highlight the significant impact of M8OI on hepatic gene expression and signal transduction pathways, elucidating the molecular mechanisms contributing to its hepatotoxicity.

https://doi.org/10.1021/envhealth.4c00120
Environ. Health 2025, 3, 373−379

Table 1. Gen Set Enrichment for Pathway BMD Based on Different Pathway Databases

Pathway	Pathway database	BMD	*P*-value	Hit gene numbers
Legionellosis	KEGG	5.9	0.011	4
Rheumatoid arthritis	KEGG	6.73	0.002	5
Transcriptional misregulation in cancer	KEGG	8.1	0.008	8
IL-17 signaling pathway	KEGG	8.29	0.002	6
Hematopoietic cell lineage	KEGG	10.38	0.005	4
Cytokine−cytokine receptor interaction	KEGG	14.79	<0.001	14
Arginine and proline metabolism	KEGG	19.32	0.011	4
Ether lipid metabolism	KEGG	44.96	0.003	4
Angiogenesis	GO BP	8.89	0.031	8
Immune response	GO BP	11.37	0.005	8
Immune system process	GO BP	15.93	0.002	14
Phospholipid metabolic process	GO BP	22.09	0.002	5
Hormone activity	GO MF	2.99	<0.001	5
Ion channel activity	GO MF	8.16	0.049	4
Cytokine activity	GO MF	11.17	<0.001	8
G protein-coupled receptor activity	GO MF	12.73	0.026	6
Plasma membrane	GO CC	10.73	0.001	75
Extracellular matrix	GO CC	11.71	0.012	8
Extracellular region	GO CC	13.92	<0.001	40
Extracellular space	GO CC	13.94	<0.001	29

3.3. Toxicogenomic Points-of-Departure and Their Implications for Risk Assessment

The benchmark dose analysis revealed that transcriptomic BMD estimates reliably predicted benchmark concentrations of M8OI-related toxicological effects. The transcriptomic BMD probability distribution curve displayed a bimodal pattern, signifying distinct concentration−response behaviors among the evaluated features (Figure 3A). Predominantly, concentration−response patterns of most transcripts converged to the Poly2 model, identifying 723 genes with a fitted model and 270 genes with determined BMDs (Figure S1). Transcriptome-wide BMD analysis identified three tPODs: omicBMD$_{20}$ at 1.51 μmol/L, omicBMD$_{10th}$ at 2.98 μmol/L, and omicBMD$_{mode}$ at 6.83 μmol/L. All three tPODs are more sensitive than the observed apical EC$_{50}$ of M8OI in HepG2 cells. OmicBMD$_{20}$ and omicBMD$_{10th}$ were highlighted as the most sensitive tPODs, derived from conservative and robust tPOD computations, independent of genome annotation.[27] Therefore, the downstream biological implications should be interpreted with caution. Conversely, omicBMD$_{mode}$ exhibited lower sensitivity than the other tPODs. Nevertheless, this value typically indicates a specific mode of action (MOA) that may hold biological relevance compared to omicBMD$_{20}$ and omicBMD$_{10th}$. This distinction facilitates elucidation of the M8OI's MOA.

The calculated pathBMD for M8OI was determined to be 5.9 μmol/L. This value was derived from the median of constitutive geneBMDs associated with the legionellosis pathway, which exhibited alterations in four genes following M8OI exposure (Table 1). Alterations in gene expression within the legionellosis pathway have been observed to fluctuate in case of liver dysfunction.[28] While the magnitude of these disturbances may be minimal, the alterations observed in the four genes within the legionellosis pathway suggested that changes in their expression may play a role in the hepatotoxicity of M8OI in HepG2 cells. Additionally, the cytokine−cytokine receptor interaction signaling pathway exhibited the highest number of constitutive geneBMDs, with 14 features demonstrating a concentration-dependent response. This suggests that while this pathway may not be the most sensitive, it is likely the most perturbed (Table 1). Inflammation serves as a critical defense mechanism against exogenous substances, particularly within the hepatic context. Dysregulation of inflammatory genes has been observed in liver inflammation induced by [C$_{14}$mim]BF$_4$ in rat models.[29] In our study, we observed alterations in key inflammatory genes, including IL1RAP, CXCL8, CXCL3 and IL-6, which are implicated in the cytokine−cytokine receptor interaction signaling pathway (Figure 3B). These findings suggested that inflammatory perturbations occurring prior to cellular injury may contribute to cell damage resulting from M8OI exposure. Furthermore, six up-regulated genes were identified (Figure 3C, highlighting their regulatory potential according to the NTP (National Toxicology Program).[30] However, caution should be exercised in interpreting these pathways regarding predicting potential apical responses induced by M8OI. It is pertinent to acknowledge that the estimation of tPODs primarily aims to identify doses or concentrations that induce biological disruption. This characterization emphasizes the apical responses arising from molecular alterations. Additionally, it is crucial for providing the evidence necessary for regulatory acceptability. These toxicogenomic points of departure have profound implications for risk assessment and further exploration into M8OI's biological impacts.

4. CONCLUSIONS

This study sheds light on the molecular mechanisms activated in human liver cells upon exposure to M8OI, providing a deeper understanding of its hepatotoxic effects. By identifying differentially expressed genes (DEGs), we offer critical insights into the pathways involved in IL-induced toxicity. These discoveries are crucial for evaluating the safety of ionic liquids and devising protective measures against their harmful impacts. Our research supports the development of safer green solvent practices, aligning with efforts to safeguard human health and the environment.

■ ASSOCIATED CONTENT

Data Availability Statement

Data will be made available on request.

Supporting Information

The Supporting Information is available free of charge at https://pubs.acs.org/doi/10.1021/envhealth.4c00120.

Description of the extensive method, Library preparation details for transcriptome sequencing, Differential expression genes (DEG) level analysis, GO and KEGG enrichment analysis of DEGs, Statistical model frequency analysis among best-fit curves (PDF)

■ AUTHOR INFORMATION

Corresponding Author

Xin Liu − *College of Food Science and Engineering, Hubei Key Laboratory for Processing and Transformation of Agricultural Products, Wuhan Polytechnic University, Wuhan*

https://doi.org/10.1021/envhealth.4c00120
Environ. Health 2025, 3, 373−379

430023, China; orcid.org/0000-0001-7689-1346; Email: liuxinhook@whpu.edu.cn

Authors

Qing Yang − *College of Food Science and Engineering, Hubei Key Laboratory for Processing and Transformation of Agricultural Products, Wuhan Polytechnic University, Wuhan 430023, China*

Xiaole Zhao − *College of Food Science and Engineering, Hubei Key Laboratory for Processing and Transformation of Agricultural Products, Wuhan Polytechnic University, Wuhan 430023, China*

Kejia Wu − *Wuxi School of Medicine, Jiangnan University, Wuxi, Jiangsu 214122, China*

Qingqing Yu − *College of Food Science and Engineering, Hubei Key Laboratory for Processing and Transformation of Agricultural Products, Wuhan Polytechnic University, Wuhan 430023, China*

Qiao Wang − *College of Food Science and Engineering, Hubei Key Laboratory for Processing and Transformation of Agricultural Products, Wuhan Polytechnic University, Wuhan 430023, China*

Jingguang Li − *NHC Key Laboratory of Food Safety Risk Assessment, Food Safety Research Unit (2019RU014) of Chinese Academy of Medical Science, China National Center for Food Safety Risk Assessment, Beijing 100021, China;* orcid.org/0000-0003-0525-7027

Yongning Wu − *College of Food Science and Engineering, Hubei Key Laboratory for Processing and Transformation of Agricultural Products, Wuhan Polytechnic University, Wuhan 430023, China; NHC Key Laboratory of Food Safety Risk Assessment, Food Safety Research Unit (2019RU014) of Chinese Academy of Medical Science, China National Center for Food Safety Risk Assessment, Beijing 100021, China;* orcid.org/0000-0001-6430-1302

Complete contact information is available at: https://pubs.acs.org/10.1021/envhealth.4c00120

Author Contributions

[⊥]Q. Yang and X.Z. contributed equally to this paper.

Author Contributions

Qing Yang: Methodology, Formal analysis, Writing-original draft. **Xiaole Zhao**: Formal analysis, Visualization, Writing-original draft. **Kejia Wu**: Investigation, Data curation, Writing-original draft. **Qingqing Yu**: Investigation, Project administration. **Qiao Wang**: Visualization, Data curation. **Jingguang Li**: Conceptualization, Resources, Writing-review and editing. **Yongning Wu**: Resources, Writing-review and editing. **Xin Liu**: Conceptualization, Supervision, Funding acquisition, Writing-review and editing.

Funding

This research was funded by the National Natural Science Foundation of China (No. 22006118) and the National Key R&D Program of China (No. 2022YFF1102500).

Notes

The authors declare no competing financial interest.

REFERENCES

(1) Singh, S. K.; Savoy, A. W. Ionic liquids synthesis and applications: An overview. *J. Mol. Liq.* **2020**, *297*, No. 112038.

(2) Wei, P.; Pan, X.; Chen, C.-Y.; Li, H.-Y.; Yan, X.; Li, C.; Chu, Y.-H.; Yan, B. Emerging impacts of ionic liquids on eco-environmental safety and human health. *Chem. Soc. Rev.* **2021**, *50* (24), 13609−13627.

(3) Toledo Hijo, A. A. C.; Maximo, G. J.; Costa, M. C.; Batista, E. A. C.; Meirelles, A. J. A. Applications of Ionic Liquids in the Food and Bioproducts Industries. *ACS Sustainable Chem. Eng.* **2016**, *4* (10), 5347−5369.

(4) Greer, A. J.; Jacquemin, J.; Hardacre, C. J. M. Industrial applications of ionic liquids. *Molecules* **2020**, *25* (21), 5207.

(5) Salar-García, M. J.; Ortiz-Martínez, V. M.; Hernández-Fernández, F. J.; de los Ríos, A. P.; Quesada-Medina, J. Ionic liquid technology to recover volatile organic compounds (VOCs). *J. Hazard. Mater.* **2017**, *321*, 484−499.

(6) Oskarsson, A.; Wright, M. C. Ionic Liquids: New Emerging Pollutants, Similarities with Perfluorinated Alkyl Substances (PFASs). *Environ. Sci. Technol.* **2019**, *53* (18), 10539−10541.

(7) Leitch, A. C.; Ibrahim, I.; Abdelghany, T. M.; Charlton, A.; Roper, C.; Vidler, D.; Palmer, J. M.; Wilson, C.; Jones, D. E.; Blain, P. G. J. T.; et al. The methylimidazolium ionic liquid M8OI is detectable in human sera and is subject to biliary excretion in perfused human liver. *Toxicology* **2021**, *459*, No. 152854.

(8) Amde, M.; Liu, J.-F.; Pang, L. Environmental Application, Fate, Effects, and Concerns of Ionic Liquids: A Review. *Environ. Sci. Technol.* **2015**, *49* (21), 12611−12627.

(9) Probert, P. M.; Leitch, A. C.; Dunn, M. P.; Meyer, S. K.; Palmer, J. M.; Abdelghany, T. M.; Lakey, A. F.; Cooke, M. P.; Talbot, H.; Wills, C.; McFarlane, W.; Blake, L. I.; Rosenmai, A. K.; Oskarsson, A.; Figueiredo, R.; Wilson, C.; Kass, G. E.; Jones, D. E.; Blain, P. G.; Wright, M. C. Identification of a xenobiotic as a potential environmental trigger in primary biliary cholangitis. *J. Hepatol.* **2018**, *69* (5), 1123−1135.

(10) Du, Z.; Zhu, L.; Dong, M.; Wang, J.; Wang, J.; Xie, H.; Zhu, S. Effects of the ionic liquid [Omim]PF6 on antioxidant enzyme systems, ROS and DNA damage in zebrafish (Danio rerio). *Aquat. Toxicol.* **2012**, *124*−*125*, 91−93.

(11) Ma, J.; Li, X.; Cui, M.; Li, W.; Li, X. J. C. Negative impact of the imidazolium-based ionic liquid [C8mim] Br on silver carp (Hypophthalmichthys molitrix): long-term and low-level exposure. *Chemosphere* **2018**, *213*, 358−367.

(12) Nan, P.; Yan, S.-g.; Wang, Y.-x.; Du, Q.-y.; Chang, Z.-j. Oxidative stress, genotoxicity and cytotoxicity of 1-methyl-3-octylimidazolium chloride on Paramisgurnus dabryanus. *Environ. Toxicol. Phar.* **2016**, *47*, 1−5.

(13) Li, X.; Ma, J.; Wang, J. Cytotoxicity, oxidative stress, and apoptosis in HepG2 cells induced by ionic liquid 1-methyl-3-octylimidazolium bromide. *Ecotox. Environ. Safe.* **2015**, *120*, 342−348.

(14) Jing, C.; Li, X.; Zhang, J.; Wang, J. Responses of the Antioxidant System in QGY-7701 Cells to the Cytotoxicity and Apoptosis Induced by 1-Octyl-3-methylimidazolium Chloride. *J. Biochem. Mol. Toxic.* **2013**, *27* (6), 330−336.

(15) Leitch, A. C.; Abdelghany, T. M.; Probert, P. M.; Dunn, M. P.; Meyer, S. K.; Palmer, J. M.; Cooke, M. P.; Blake, L. I.; Morse, K.; Rosenmai, A. K.; Oskarsson, A.; Bates, L.; Figueiredo, R. S.; Ibrahim, I.; Wilson, C.; Abdelkader, N. F.; Jones, D. E.; Blain, P. G.; Wright, M. C. The toxicity of the methylimidazolium ionic liquids, with a focus on M8OI and hepatic effects. *Food Chem. Toxicol.* **2020**, *136*, No. 111069.

(16) Leitch, A. C.; Abdelghany, T. M.; Charlton, A.; Grigalyte, J.; Oakley, F.; Borthwick, L. A.; Reed, L.; Knox, A.; Reilly, W. J.; Agius, L. J. E.; Safety, E.; et al. Renal injury and hepatic effects from the methylimidazolium ionic liquid M8OI in mouse. *Ecotox. Environ. Safe.* **2020**, *202*, No. 110902.

(17) Alcaraz, A. J. G.; Mikulášek, K.; Potěšil, D.; Park, B.; Shekh, K.; Ewald, J.; Burbridge, C.; Zdráhal, Z.; Schneider, D.; Xia, J.; Crump, D.; Basu, N.; Hecker, M. Assessing the Toxicity of 17α-Ethinylestradiol in Rainbow Trout Using a 4-Day Transcriptomics Benchmark Dose (BMD) Embryo Assay. *Environ. Sci. Technol.* **2021**, *55* (15), 10608−10618.

(18) Essfeld, F.; Ayobahan, S. U.; Strompen, J.; Alvincz, J.; Schmidt-Posthaus, H.; Woelz, J.; Mueller, T.; Ringbeck, B.; Teigeler, M.; Eilebrecht, E.; Eilebrecht, S. Transcriptomic Point of Departure (tPOD) of androstenedione in zebrafish embryos as a potential surrogate for chronic endpoints. *Sci. Total Environ.* **2024**, *953*, No. 176026.
(19) Haber, L. T.; Dourson, M. L.; Allen, B. C.; Hertzberg, R. C.; Parker, A.; Vincent, M. J.; Maier, A.; Boobis, A. R. Benchmark dose (BMD) modeling: current practice, issues, and challenges. *Crit. Rev. Toxicol.* **2018**, *48* (5), 387−415.
(20) Ewald, J.; Soufan, O.; Xia, J.; Basu, N. FastBMD: an online tool for rapid benchmark dose−response analysis of transcriptomics data. *Bioinformatics* **2021**, *37* (7), 1035−1036.
(21) Thamke, V.; Singh, P.; Pal, S.; Chaudhary, M.; Kumari, K.; Bahadur, I.; Varma, R. S. Current toxicological insights of ionic liquids on various environmental living forms. *J. Environ. Chem. Eng.* **2022**, *10* (2), No. 107303.
(22) Stolte, S.; Arning, J.; Bottin-Weber, U.; Müller, A.; Pitner, W.-R.; Welz-Biermann, U.; Jastorff, B.; Ranke, J. Effects of different head groups and functionalised side chains on the cytotoxicity of ionic liquids. *Green Chem.* **2007**, *9* (7), 760−767.
(23) Arning, J.; Matzke, M. J. C. O. C. Toxicity of ionic liquids towards mammalian cell lines. *Curr. Org. Chem.* **2011**, *15* (12), 1905−1917.
(24) Ma, S.; Xiao, Y.; Zhang, X.; Xu, Y.; Zhu, K.; Zhang, K.; Li, X.; Zhou, H.; Chen, G.; Guo, X. Dietary exposure to polystyrene microplastics exacerbates liver damage in fulminant hepatic failure via ROS production and neutrophil extracellular trap formation. *Sci. Total Environ.* **2024**, *907*, No. 167403.
(25) Yang, W.; Ling, X.; He, S.; Cui, H.; Yang, Z.; An, H.; Wang, L.; Zou, P.; Chen, Q.; Liu, J.; Ao, L.; Cao, J. PPARα/ACOX1 as a novel target for hepatic lipid metabolism disorders induced by per- and polyfluoroalkyl substances: An integrated approach. *Environ. Inter.* **2023**, *178*, No. 108138.
(26) Li, N.; Yamamoto, G.; Fuji, H.; Kisseleva, T. Interleukin-17 in liver disease pathogenesis. *Semin Liver Dis* **2021**, *41*, 507−515.
(27) Pagé-Larivière, F.; Crump, D.; O'Brien, J. M. Transcriptomic points-of-departure from short-term exposure studies are protective of chronic effects for fish exposed to estrogenic chemicals. *Toxical. Appl. Pharm.* **2019**, *378*, No. 114634.
(28) Jomehzadeh, N.; Moosavian, M.; Saki, M.; Rashno, M. Legionella and legionnaires' disease: An overview. *J. Acute Dis.* **2019**, *8* (6), 221.
(29) Yuan, H.; Xu, F.; Tian, X.; Wei, H.; Zhang, R.; Ge, Y.; Xu, H. Oxidative stress and inflammation caused by 1-tetradecyl-3-methylimidazolium tetrafluoroborate in rat livers. *Environ. Sci. Pollut. R* **2022**, *29* (57), 86680−86691.
(30) National Toxicology Program. *NTP research report on national toxicology program approach to genomic dose-response modeling*; National Toxicology Program: Durham, NC, 2018.

https://doi.org/10.1021/envhealth.4c00120
Environ. Health 2025, 3, 373−379